Benemérita Universidad Autónoma de Puebla

Facultad de Ciencias Físico Matemáticas

The redshift of test particles orbiting nonsingular black holes in conformal gravity

Thesis presented to

Colegio de Física

in partial fulfillment of the requirement for the degree

LICENCIADO EN FÍSICA

by

Diego Armando Martínez Valera

Thesis advisors:

Dr. Mehrab Momennia
Dr. Cupatitzio Ramírez Romero

Puebla Pue.
March 2024

Benemérita Universidad Autónoma de Puebla

Facultad de Ciencias Físico Matemáticas

The redshift of test particles orbiting nonsingular black holes in conformal gravity

Thesis presented to

Colegio de Física

in partial fulfillment of the requirement for the degree

LICENCIADO EN FÍSICA

by

Diego Armando Martínez Valera

Thesis advisors:

Dr. Mehrab Momennia
Dr. Cupatitzio Ramírez Romero

Puebla Pue.
March 2024

Title: The redshift of test particles orbiting nonsingular black holes in conformal gravity
Student: DIEGO ARMANDO MARTÍNEZ VALERA

COMMITTEE

Dr. Gerardo Francisco Torres del Castillo
President

Dr. Alfredo Herrera Aguilar
Secretary

Dra. Mercedes Paulina Velázquez Quesada
Vocal

Dr. Roberto Cartas Fuentevilla
Vocal

Dr. Mehrab Momennia
Dr. Cupatitzio Ramírez Romero
Advisors

Contents

Dedications

A mis padres, mi hermano y mis sobrinos, por haberme brindado todo su apoyo incondicional, por su cariño y por llenar mi vida de alegría, sirviéndome de inspiración.

Acknowledgments

I would like to thank all the support, the guidance, and the patience from my advisors, Dr. Mehrab Momennia and Dr. Cupatitzio Ramirez, for sharing their time and knowledge with me. I also would like to thank Dr. Alfredo Herrera Aguilar for his support and valuable comments. To the members of the committee for their valuable comments and their time. To my family who has always been supportive, for rising me with unconditional love and patience, and for bringing joy and direction to my life. To all the friends who have been along with me, giving me advice, and for all the good times.

For this and many more things, I would like to thank them all, to be part of this journey and to share their knowledge.

Abstract

In this thesis, we obtain an expression for the total frequency shift (hereafter called total observational frequency shift, since it refers to the frequency shift obtained from observable data of astrophysical systems) of photons emitted by massive particles in geodesic motion circularly orbiting a black hole in a general spherically symmetric background. Our general relations are presented in terms of the metric components and their derivatives that characterize the black hole parameters. As a concrete example of this general relativistic approach, a special case is studied by applying the formalism to a nonsingular black hole conformally related to the Schwarzchild solution that possesses a length scale parameter l and an integer parameter N in addition to the black hole mass. Besides, we express the nonsingular black hole mass in terms of the observational redshift/blueshift. Finally, we investigate the effects of the free parameters of the conformal gravity theory on the observational frequency shift and compare results with those of the standard Schwarzschild black hole.

Introduction

In the last century, we have witnessed important advances in understanding our universe, switching from the old Newtonian picture to a more profound view. These new ideas that revolutionized physics have their fundamentals based on the theory of relativity, which consists of the Special Theory of Relativity (SR) and the General Theory of Relativity (GR). Both theories were some of the greatest developments of physics in the early 20^{th} century alongside quantum mechanics, giving a new perspective of the universe from the microscopic to the cosmological scale and setting the stage for further developments in cosmology and astrophysics.

SR invented by Einstein and presented on September 26, 1905, in the paper entitled "*On the electrodynamics of moving bodies*" as a result of some inconsistencies in classical physical theory and the problem of dealing with the idea of *aether*, which was thought of as a hypothetical propagation medium for electromagnetic waves. Nevertheless, with the unfruitful results of Michelson and Morley's experiment, this aether concept began to be questioned.

This is where SR plays its role to get rid of the concept of aether and absolute space, stating there is no a privileged inertial reference frame. Therefore, all physical laws must remain the same in all inertial reference frames. Another important fact remarked by SR is that the speed of light *in vacuo* must be the same for all inertial reference frames. These two facts were stated as the two postulates of SR, which gave rise to all the consequences found in the theory, such as the spacetime unity, time dilation, and length contraction, just to mention a few examples. Once the theory was being deeply studied, physicists looked for a generalization of the developed concepts in SR that led to the appereance of GR in the scene.

GR was introduced by Einstein in 1915 as the generalization of SR to spacetimes in the presence of gravitational fields. This theory of gravitation is constructed based on SR notions and the Equivalence Principle which states that an accelerated reference frame in the absence of gravity is equivalent to the same reference frame at rest in the presence of gravity.

This new picture of gravitation changed the perspective of the gravitational force to spacetime curvature produced by the presence of matter and energy. The concept of curvature plays a central role in the theory and it is characterized by the Riemann tensor $R^{\alpha}{}_{\mu\beta\nu}$ which is expressed in terms of Christoffel symbol $\Gamma^{\mu}_{\nu\sigma}$ and its partial derivatives, and in turn, $\Gamma^{\mu}_{\nu\sigma}$ is expressed in terms of partial derivatives of the metric $g_{\mu\nu}$ (see Eqs. (A.1) and (A.3) of the Appendix).

The validity of GR has been supported so far by several observational tests, such as perihelion precession of Mercury, deflection of light, gravitational redshift, gravitational lensing, the equivalence principle, detection of gravitational waves, and black hole shadow. GR is governed by the Einstein field equations

$$G_{\mu\nu} = \frac{8\pi G}{c^4} T_{\mu\nu}. \tag{1}$$

Here G =6.67$\times 10^{-11} m^3 s^{-2} kg^{-1}$ is the universal gravitational constant and $c = 3 \times 10^8 ms^{-1}$ is the speed of light in the vacuum. In the left-hand side (lhs) of the field equations, the Einstein tensor $G_{\mu\nu}$ is defined as follows

$$G_{\mu\nu} = R_{\mu\nu} - \frac{1}{2} g_{\mu\nu} R, \tag{2}$$

where $R_{\mu\nu} = g_{\alpha\rho} g^{\rho\beta} R^{\alpha}{}_{\mu\beta\nu}$ is the Ricci tensor and $R = g_{\mu\nu} R^{\mu\nu}$ is the scalar curvature. The field equations (1) in terms of such expressions become a set of nonlinear second order partial differential equations, where the right-hand side (rhs) $T_{\mu\nu}$ is the energy-momentum tensor which depends on the matter source.[1]

Just about two months after publication of Einstein's results, Karl Schwarzschild obtained the first solution to the field equations. He assumed the case of a spherical non-rotating star and found that for an exterior solution (outside the massive body where $T_{\mu\nu} = 0$), the metric $g_{\mu\nu}$ that describes the spacetime has the form

$$ds^2 = g_{\mu\nu} x^\mu x^\nu = -\left(1 - \frac{2GM}{c^2 r}\right) c^2 dt^2 + \left(1 - \frac{2GM}{c^2 r}\right)^{-1} dr^2 + r^2 d\theta^2 + r^2 \sin^2\theta d\varphi^2, \tag{3}$$

expressed in spherical coordinates for simplicity due to the spherical symmetry of the problem. First, we see that there exist a couple of points in which Eq. (3) diverges, hence the line element posses singularities at $r = 0$ and $r_s = \frac{2GM}{c^2}$. The latter is known as *Schwarzschild radius*[2] which defines a region of spacetime called *event horizon* and denoted by r_s.

In addition, one can notice that by employing a change in the coordinate system[3], the coordinate singularity r_s can be eliminated. On the other hand, in spite of our coordinate system election, the singularity corresponding to $r = 0$ will remain, which is known as the intrinsic (curvature) singularity due to the fact that the curvature tensor diverges at this point as well. The metric function $(1 - \frac{r_s}{r})$ at spatial infinity $(r \to \infty)$ tends to 1, and therefore the Schwarzschild metric (3) reduces to

$$\begin{aligned} ds^2 &= -c^2 dt^2 + dr^2 + r^2 d\theta^2 + r^2 \sin^2\theta d\varphi^2 \\ &= -c^2 dt^2 + dx^2 + dy^2 + dz^2 = \eta_{\mu\nu} dx^\mu dx^\nu, \end{aligned} \tag{4}$$

which is the line element for the Minkowski spacetime and $\eta_{\mu\nu} = diag(-1, 1, 1, 1)$ is the Minkowski metric in the cartesian coordinates $x^\mu = (ct, x, y, z)$. Hence, the Schwarzschild spacetime reduces to the Minkowski line element for large enough values of the radial coordinate r. This means the spacetime produced by static spherical massive objects becomes flat far enough from the source and such backgrounds are known as asymptotically flat spacetimes. It is important to point out that due to the spacetime metric, the r coordinate is related to the radial distance by[4]

$$\text{distance} = \int_a^b \sqrt{g_{rr}} dr = \int_a^b \frac{dr}{\sqrt{1 - \frac{r_s}{r}}}. \tag{5}$$

Another important feature of GR is that we can obtain the following expression for the line element of an observer at rest $(dr = d\theta = d\varphi = 0)$

$$ds^2 = c^2 g_{tt} dt^2, \tag{6}$$

and by considering the relation $ds^2 = -c^2 d\tau^2$, we obtain the proper time τ as follows

$$\tau = \int_0^{t_0} \sqrt{-g_{tt}}\, dt, \tag{7}$$

where in the case of the Schwarzschild spacetime we have $g_{tt} = -\left(1 - \frac{r_s}{r}\right)$, and for this particular metric, the proper time corresponds to the time registered by an observer at infinity $r \to \infty$, $\tau = t_0$.

We recall that the Schwarzschild solution to Einstein equations is valid outside the surface of usual stellar massive objects such as a star. However, if we consider the case of a compact object such that its

[1] Note that due to the nonlinearity of the field equations, GR does not obey the superposition principle, in contrast to the Newtonian theory of gravitation.

[2] For stars like the Sun, the Schwarzschild radius lies inside them. The Sun's radius is approximately 6.85×10^6km and its Schwarzschild radius is about 2.9 km.

[3] Take, e.g. the change of coordinates $r* = ct + r + \frac{2GM}{c^2} ln|\frac{c^2 r}{2GM} - 1|$, known as Eddington-Finkelstein coordinates.

[4] Further details and the procedure to obtain the Schwarzschild solution to Eq. (1) can be found in most GR textbooks, for instance, see [1, 2].

radius lies inside the Schwarzschild radius, we can also analyze the spacetime for the inner region $r < r_s$ where the vacuum Einstein field equations are still valid. In this case, it is necessary to pay attention to the hypersurface $r = r_s$ and its physical implications.

The event horizon is just a coordinate singularity located at $r = r_s$ where the spacetime is well-behaved, and therefore, any particle can pass through it without trouble. But, it turns out that once a particle crosses the event horizon, it cannot escape that region of spacetime, and once gets inside the Schwarzschild radius, the particle necessarily ends up falling into the essential singularity at $r = 0$.

Black holes are one of the most important results of GR while it is difficult to deal with them by means of direct measurements of their parameters, such as mass, angular momentum, and electric charge. In fact, several decades of theoretical and technological developments were necessary to finally obtain observational evidence of the existence of black holes based on reliable data. From the theoretical point of view, there was a debate on the prediction of singularities in the solutions of Einstein equations. It was believed that the spherically symmetry was a necessary condition for having gravitational collapse, otherwise for a non-spherically symmetric spacetime, it seemed improbable that in-falling matter concentrated into a single point would create a singularity.

The problem of gravitational collapse was addressed by Roger Penrose [3] who decided to analyze the issue by assuming that collapsing matter had positive energy density, without the assumption of spherical symmetry. With the aid of some mathematical tools, he was able to study the causal structure of a black hole, concluding that the event horizon exists regardless of the type of solution taken into account and its associated symmetry. He emphasized the importance of the event horizon as a main feature that defines a black hole, since it determines the no-returning point for a particle travelling to the inner region where the space direction becomes timelike, making impossible for the particle to turn back and escape, hence falling towards the singularity at $r = 0$.

Some believed that nature would protect itself from creating singularities, and that an arbitrary distribution of matter and gravitational field does not lead to the appearance of a singularity. However, in the early 1960s, compact radio sources (originally thought to be stars and regarded as quasi-stellar objects or quasars, for short) with no optical counterpart were detected. Nevertheless, further observations rendered by Schmidt from extragalactic compact radio sources located outside the Milky Way galaxy, revealed that these radio sources might correspond to compact and very massive sources of energy, and not to "star-like" sources [4]. These quasars were considered to be in the center of what is known as Active Galactic Nuclei (AGNs) instead of being isolated objects. As a result of these discoveries, an explanation for quasars' observations was needed. Independently, it has been argued that nuclear mechanisms in stars produce a gravitational contraction for large enough densities, and therefore, it is possible to have black holes in nature under certain conditions [5]. As a result, it was proposed that a growth in mass of a black hole due to accretion of interstellar gas onto it would generate a *supermassive black hole* that can explain the quasars detections. This idea was supported by observational evidence that suggests the presence of extremely massive compact objects with a mass of the order $10^6 M_\odot - 10^9 M_\odot$[5] hosted in the galaxy centers.

In this regard, two teams of astronomers, led by Genzel and Ghez, obtained observational data by monitoring the star orbits in the galactic center for almost three decades which yields evidence supporting the existence of dense compact objects [6–8]. In addition, more recently, strong evidence has been provided by the shadow images of supermassive black holes hosted at the center of M87 and the Milky Way galaxies revealed by the Event Horizon Telescope [9, 10] as well as gravitational wave detection from LIGO-Virgo collaborations [11, 12].

A brief review of the general relativistic formalism for frequency shift

The method used in this thesis takes into account the redshift/blueshift obtained by analyzing the spectral lines of light emitted by a massive particle circularly orbiting a black hole within the framework of GR. This method has been introduced and developed in [13–17] with the aim of measuring the black hole and

[5] $M_\odot = 2 \times 10^{30}$kg is the solar mass.

cosmological parameters. The motivation for the development of this general relativistic approach is the evidence of the presence of supermassive black holes hosted in the center of spiral galaxies, such as the case of SgrA* at the center of our galaxy.

This formalism has been constructed taking into account the geodesic motion of massive light emitters (such as stars or gas particles) circularly orbiting black holes and with the help of the nonvanishing components of their 4-velocity and the 4-wave vector of the emitted photons as well as conserved quantities obtained by identifying the symmetries of the spacetime. With the help of this general relativistic approach and in the case of rotating Kerr black holes, one can obtain expressions for the black hole mass and spin in terms of the directly observable redshift/blueshift as well as the orbital parameter of the emitter [14]. However, in the particular case of spherically symmetric spacetimes, it is possible to set the emitter orbits in the equatorial plane without loss of generality [16]. This method has been also employed to express the parameters of static polymerized black holes in terms of the total redshift [18]. In addition, it was shown that by employing a similar procedure, it is possible to extract the Hubble law from the Kerr black hole in asymptotically de Sitter spacetime and add a new independent general relativistic approach to measure the late-time Hubble constant [15].

In addition, one can apply this general relativistic formalism to real astrophysical systems with available data on the frequency shift and positions of orbiting particles. This method has been used so far to estimate the mass-to-distance ratio of 17 supermassive black holes in the center of active galactic nuclei (AGNs) which possess an accretion disk of water vapor clouds [19–22]. It was demonstrated that this relativistic approach allows us to quantify the gravitational redshift, hence identifying the relativistic effects in such astrophysical systems. Recently, by introducing the "redshift rapidity" which is an observable element, we disentangled M and D in the Schwarzschild black hole spacetime and expressed mass and distance to the black hole just in terms of observational frequency shifts [17].

This thesis is outlined as follows: In Chapter 1, we present a general review of conformal gravity and give a brief overview of the nonsingular spacetimes generated from the Schwarzschild black hole solutions undergoing a conformal transformation. In Chapter 2, an analysis of the geodesic motion of massive and massless particles in a general spherically symmetric spacetime is carried out. Besides, we express the nonvanishing 4-velocity components of these particles by taking into account the conserved quantities associated to Killing vector fields of the spacetime. Then in Chapter 3, using the results of Chapter 2, we derive an expression for total observational frequency shift for massive particles orbiting a black hole in a general spherical symmetric spacetime. In Chapter 4, as an application of this general formalism, we obtain the frequency shift of the nonsingular black holes in conformal gravity introduced in Chapter 1 and analyze the behavior of redshift/blueshift versus the black hole parameters. Then, we will present some analytic exact formulas for the nonsingular black hole mass in terms of observational redshift and orbital parameters of the emitter. Finally, some concluding remarks are presented in Chapter 5.

Chapter 1

Nonsingular black holes in conformal gravity

Einstein's theory of gravity is currently the most accurate theory which describes with an excellent precision gravitational phenomena in the Universe. However, it suffers from some ambiguities such as the prediction of singularities like those present in the center of black holes. These regions of spacetime are currently unknown, we do not possess information on the behaviour of physics laws in such extreme conditions since they appear at huge energy densities where the bending of spacetime is too strong and the predictability of the theory is not reliable anymore. In such conditions, we tend to believe that a quantum description of gravity is necessary to describe points near the singularity. Nevertheless, there is no self-consistent and complete quantum theory of gravity so far.

The resolution of spacetime singularities has been a longstanding problem, addressed by authors with different approaches, such as extending the gravitational theory beyond general relativity. Within the wide variety of proposals in the literature, conformally invariant theories of gravitation [1] seem to overcome the singularity issue very neatly.

Taking this into account, we focus on conformal gravity theories, which are based on rescaling the metric $g_{\mu\nu}$ by the conformal factor Ω as follows

$$g_{\mu\nu} \to \Omega^2(x) g_{\mu\nu}, \tag{1.1}$$

where $\Omega(x)$ is a function of the spacetime coordinates.

Nevertheless, in contrast to some other theories such as the case of Maxwell's electromagnetic theory, classical GR is not conformally invariant. This can be seen from the transformation law of the Ricci tensor under a conformal rescaling of the form (1.1) [23]

$$\hat{R}_{\mu\nu} = R_{\mu\nu} + \frac{2}{\Omega}\nabla_\mu\nabla_\nu\Omega + g_{\mu\nu}g^{\rho\sigma}\left(\frac{1}{\Omega}\nabla_\rho\nabla_\sigma\Omega - \frac{3}{\Omega^2}\nabla_\rho\Omega\nabla_\sigma\Omega\right), \tag{1.2}$$

where $\hat{R}_{\mu\nu}$ is associated to the metric $\hat{g}_{\mu\nu}$, and we see that the expression is singular for $\Omega = 0$.

This issue has been solved by taking into account Weyl conformal symmetry. In this regard, one can construct a conformally invariant theory from the following action [24]

$$I_{Universe} = I_{Matter} + I_{Weyl} = -\alpha_g \int d^4x(-g)^{1/2} C_{\mu\nu\rho\sigma}C^{\mu\nu\rho\sigma} + I_{Matter}, \tag{1.3}$$

where the I_{Matter} and I_{Weyl} terms stand for the matter source and Weyl action, respectively; α_g is a dimensionless coupling constant, $g = det[g_{\mu\nu}]$, and $C_{\mu\nu\rho\sigma}$ is the Weyl tensor defined as follows in 4-

[1] The light cones and some physical laws preserve under conformal transformations [23].

dimensional spacetime

$$C_{\mu\nu\rho\sigma} = R_{\mu\nu\rho\sigma} + \frac{1}{6}R[g_{\mu\rho}g_{\nu\sigma} - g_{\mu\sigma}g_{\nu\rho}] - \frac{1}{2}[g_{\mu\rho}R_{\nu\sigma} - g_{\mu\sigma}R_{\nu\rho} - g_{\nu\rho}R_{\mu\sigma} + g_{\nu\sigma}R_{\mu\rho}], \tag{1.4}$$

which is invariant under conformal rescaling that leads to the conformal invariance of the action (1.3). Hence, the integrand in Eq. (1.3) can be expressed in terms of the Riemann tensor, Ricci tensor, and Ricci scalar as follows

$$C_{\mu\nu\rho\sigma}C^{\mu\nu\rho\sigma} = R_{\mu\nu\rho\sigma}R^{\mu\nu\rho\sigma} - 2R_{\nu\rho}R^{\nu\rho} + \frac{1}{3}R^2. \tag{1.5}$$

Furthermore, the Weyl tensor (1.4) vanishes for the metric contraction of any pair of indices, for example

$$g^{\nu\sigma}C^{\mu}_{\nu\rho\sigma} = 0. \tag{1.6}$$

Moreover, conformal transformations (1.1) differ from a conformal coordinate transformation

$$x \longrightarrow x' \tag{1.7}$$

$$g_{\mu\nu} \longrightarrow \Omega^2(x')g_{\mu\nu}(x'), \tag{1.8}$$

which apart from the factor Ω^2, involves a coordinate transformation, whereas a conformal transformation of the form (1.1) changes the length scales, but not angles.

Therefore, for a given metric, a new spacetime can be generated by employing a conformal transformation. This new spacetime $\hat{g}_{\mu\nu}$ is said to be conformally related to the former background $g_{\mu\nu}$ if it satisfies the following relation [25]

$$\hat{g}_{\mu\nu} = \Omega^2\, g_{\mu\nu}, \tag{1.9}$$

where it is assumed that the conformal factor Ω is a twice differentiable function of the spacetime coordinates and satisfies $0 < \Omega$.

It is easy to see that conformal transformations preserve angles by taking into account the expression for an angle θ subtended by the vectors A^μ and B^ν

$$\cos\theta = \frac{g_{\mu\nu}A^\mu B^\nu}{|A||B|} = \frac{g_{\mu\nu}A^\mu B^\nu}{\sqrt{(g_{\alpha\beta}A^\alpha A^\beta)(g_{\rho\sigma}B^\rho B^\sigma)}}, \tag{1.10}$$

then, by applying a conformal mapping of the form (1.9), the expression for an angle θ' subtended by two vectors $\tilde{A}^\mu$ and $\tilde{B}^\mu$ yields

$$\cos\theta' = \frac{\hat{g}_{\mu\nu}\tilde{A}^\mu\tilde{B}^\nu}{|\tilde{A}||\tilde{B}|} = \frac{\Omega^2 g_{\mu\nu}A^\mu B^\nu}{\Omega^2|A||B|} = \cos\theta. \tag{1.11}$$

From a physical point of view, it is expected that in high curvature regimes, conformal symmetry is preserved by Nature, which chooses a conformal theory among the family of conformal invariant gauges [26, 27]. The Universe does not appear to possess conformal invariance, nonetheless, there are theoretical models which support scale invariance in the early Universe [26, 28, 29].

Such evidence suggests the existence of conformal symmetry at high curvature regimes. Hence, by assuming that conformal symmetry is indeed present in Nature, there must occur a spontaneous symmetry breaking process. Therefore, in the phase where this process takes place, Nature is expected to select a conformal gauge (related to a conformal factor Ω) which gives rise to a regular spacetime.

Then, in order to solve the singularity problem of the Schwarzschild metric, we can turn our attention to the conformal symmetry and build metrics that are conformally equivalent to the Scharzschild spacetime, *i.e.* finding a suitable function Ω depending on the spacetime coordinates such that Eq. (1.9) holds.

In this work, instead of considering a specific conformal gravity theory, we focus on a family of conformal transformations by following [26, 30]. In this way, singularities can be eliminated by a suitable conformal mapping, and for this purpose, the following conformal factor has been proposed [26, 30]

$$\Omega^2(r) = \left(1 - \frac{l^2}{r^2}\right)^{2N}, \tag{1.12}$$

where l is a length scale parameter and N is a positive integer. Note that the conformal factor $\Omega^2(r)$ satisfies $\Omega^{-2}(0) = 0$ as well as $\Omega^{-2}(\infty) = 1$.

In this context, conformal gravity is an extended theory of gravitation that provides a way to get rid of singularities by means of a conformal transformation of the form (1.9) applied to the Schwarzschild metric $g_{\mu\nu}$, giving rise to a new metric $\hat{g}_{\mu\nu}$ which is conformally related to $g_{\mu\nu}$. In this regard, one assigns the conformal symmetry to the Schwarzschild background, hence the spacetime singularity can be removed after a suitable conformal transformation. Nonsingular black holes conformally related to the Scharzschild solutions and the Kerr solutions have been proposed in [26, 30], in which their spacetime is geodesically complete. In this thesis, we employ the conformal factor (1.12) to define the new spacetime based on the Schwarzschild solutions[2]

$$d\hat{s}^2 = \Omega^2(r) ds^2 = \left(1 - \frac{l^2}{r^2}\right)^{2N} \left[-\left(1 - \frac{2M}{r}\right) dt^2 + \frac{1}{\left(1 - \frac{2M}{r}\right)} dr^2 + r^2 d\theta^2 + r^2 \sin^2\theta d\varphi^2 \right], \tag{1.13}$$

hence, the metric components read

$$\hat{g}_{tt} = -f(r) = -\left(1 - \frac{l^2}{r^2}\right)^{2N} \left(1 - \frac{2M}{r}\right), \tag{1.14}$$

$$\hat{g}_{rr} = \left(1 - \frac{l^2}{r^2}\right)^{2N} \left(1 - \frac{2M}{r}\right)^{-1}, \tag{1.15}$$

$$\hat{g}_{\theta\theta} = \left(1 - \frac{l^2}{r^2}\right)^{2N} r^2, \tag{1.16}$$

$$\hat{g}_{\varphi\varphi} = \left(1 - \frac{l^2}{r^2}\right)^{2N} r^2 \sin^2\theta. \tag{1.17}$$

This metric characterizes a nonsingular black hole conformally equivalent to the Schwarzschild black hole. Further, one can readily verify that this metric is asymptotically flat since $\lim_{r\to\infty} \Omega^2(r) = 1$. The fact that this new metric represents a nonsingular spherically symmetric black hole is because its spacetime is geodesically complete and the curvature invariants are regular everywhere [26, 30].

On the one hand, geodesic completeness refers to the property of a pseudo-Riemannian manifold for which starting at a point p, it is possible to follow a straight line for an infinite amount of its proper time/affine parameter. On the other hand, one can show that the rescaled spacetime does not possess divergencies by computing the Ricci scalar [26, 31]

$$R \approx \frac{24N^2}{l^{4N}} r^{4N-3}, \tag{1.18}$$

and the Kretschmann scalar

$$\mathcal{K} \approx \frac{12(1 + 12N^2 - 16N^3 + 16N^4)}{l^{8N}} r^{8N-6}, \tag{1.19}$$

in the limit $r \to 0$ where the black hole singularity usually takes place.

One notices that as long as $l \neq 0$ and $N \geq 1$, R and $\mathcal{K}$ are continuous which means once the conformal transformation is applied to the Schwarzschild metric, the resulting spacetime does not possess curvature singularities. This fact alongside the geodesic completeness of the new spacetime suggests that we are dealing with a singularity-free background. It is worth noting that curvature singularities are different from geodesic singularities and in general, studying the former does not ensure the regularity of spacetime.

[2] Note that we recover the Schwarzschild spacetime for $l = 0$ and/or $N = 0$.

It is also worth mentioning that the conformal factor presented in the line element (1.13) can be obtained as part of the solution to Einstein field equations (1) by considering the effective energy-momentum tensor of an anisotropic fluid of the form [31]

$$T_{\mu\nu} = (\rho + p_2)U_\mu U_\nu + (p_1 - p_2)x_\mu x_\nu + p_2 \hat{g}_{\mu\nu}, \tag{1.20}$$

where p_1 and p_2 are the radial and tangential pressure, respectively, ρ is the energy density measured by a comoving observer with the fluid, U_μ is the 4-velocity, and x_μ is a spacelike unit vector ($x_\mu x^\mu = 1$). For a comoving observer, we have $U^\mu = (U^t, 0, 0, 0)$ and $x^\mu = (0, x^r, 0, 0)$, therefore, the components of the energy-momentum tensor are written in the following way

$$T_{tt} = -\hat{g}_{tt}\rho, \tag{1.21}$$

$$T_{rr} = \hat{g}_{rr}p_1, \tag{1.22}$$

$$T_{\theta\theta} = \hat{g}_{\theta\theta}p_2, \tag{1.23}$$

$$T_{\varphi\varphi} = \hat{g}_{\varphi\varphi}p_2. \tag{1.24}$$

In this alternative description where the Schwarzschild metric is multiplied by the conformal factor (1.12), the explicit expressions of ρ, p_1, and p_2 are functions of r that can be obtained by calculating the corresponding Einstein tensor $G_{\mu\nu}(\hat{g})$ constructed from the metric (1.13).

Chapter 2

Geodesic motion in a general spherically symmetric spacetime

From Euclidean geometry, we know that the shortest path between two points in a flat space is a straight line. However, when we try to generalize this idea to curved spaces, we find that this is no longer true. In this sense, geodesics can be thought of as the 'shortest path' that a particle can follow in spacetime. The problem of finding geodesic curves can be addressed mathematically using the Lagrangian formalism in the following way.

Consider the Lagrangian [1, 2]

$$\mathcal{L} = g_{\mu\nu}\dot{x}^{\mu}\dot{x}^{\nu}, \tag{2.1}$$

where $\dot{x}^{\mu} = \frac{dx^{\mu}}{d\lambda}$ denotes the derivative of the particle's position where λ is the affine parameter for photons and it represents the proper time $\lambda = \tau$ in the case of massive particles. Now, similarly to the least action principle in classical mechanics, we can find the shortest path that the test particle takes between two points. This can be performed by varying the action constructed with the Lagrangian density given in Eq. (2.1) and setting it equal to zero, which yields the Euler-Lagrange equations. Hence, the problem reduces to apply Euler-Lagrange equations to Eq. (2.1), which leads to the geodesic equation (see [1] for details of calculations)

$$\ddot{x}^{\mu} + \Gamma^{\mu}_{\gamma\delta}\,\dot{x}^{\gamma}\dot{x}^{\delta} = 0. \tag{2.2}$$

In addition, in what follows we take into account a general static and spherically symmetric black hole background with a flat asymptote. The line element takes the following form in the Schwarzschild coordinates (t, r, θ, φ)[1,2]

$$ds^2 = g_{\mu\nu}dx^{\mu}dx^{\nu} = g_{tt}dt^2 + g_{rr}dr^2 + g_{\theta\theta}d\theta^2 + g_{\varphi\varphi}d\varphi^2 = -f(r)dt^2 + g(r)dr^2 + h(r)[d\theta^2 + \sin^2\theta\, d\varphi^2], \tag{2.3}$$

where the metric functions $f(r)$, $g(r)$, and $h(r)$ satisfy

$$\lim_{r\to\infty} f(r) = 1, \quad \lim_{r\to\infty} g^{-1}(r) = 1, \quad \lim_{r\to\infty} h(r) = r^2, \tag{2.4}$$

This implies that the spacetime described by the line element in Eq. (2.3) is asymptotically flat, and therefore, the curved spacetime takes the form of Minkowski flat spacetime (4) when r tends to infinity. Hereafter, we remove the argument r from the metric functions for notational simplicity.

---

[1] In natural units we set $c = 1 = G$.

[2] We normally use the term *spherical coordinates* for the spatial coordinates r, θ and φ, but here we take the time t as part of the generalization of spherical coordinates in the 4-dimensional spacetime.

Then, the trajectory of particles revolving around the spherically symmetric background (2.3) is governed by the following equation of motion, which is equivalent to Eq. (2.2)

$$\frac{ds^2}{d\lambda^2} = g_{\mu\nu}\dot{x}^\mu \dot{x}^\nu = \kappa, \tag{2.5}$$

for both timelike ($\kappa = -1$) and null ($\kappa = 0$) world lines.

2.1 Massive particles

In the case of massive particles, one can take the parameter λ to be the proper time τ, hence Eq. (2.5) leads to

$$\frac{ds^2}{d\tau^2} = g_{\mu\nu}\dot{x}^\mu \dot{x}^\nu = g_{\mu\nu}U^\mu U^\nu = g_{tt}(U^t)^2 + g_{rr}(U^r)^2 + g_{\theta\theta}(U^\theta)^2 + g_{\varphi\varphi}(U^\varphi)^2 = -1. \tag{2.6}$$

where $U^\mu \equiv dx^\mu/d\tau$ is the 4-velocity of the particle

$$U^\mu = (U^t, U^r, U^\theta, U^\varphi). \tag{2.7}$$

For the study of geodesic particles is convenient to take into account the symmetries of the spacetime, due to their relation to conserved quantities. In this regard, it is worth noting that a coordinate basis vector $\partial_\alpha \equiv \frac{\partial}{\partial x^\alpha}$ associated with a cyclic coordinate x^α of the Lagrangian given in Eq. (2.1) yields a conserved quantity (see section 6.11 of [32] for a deeper discussion of this topic). By expressing Eq. (2.2) in terms of the 4-momentum

$$p^\mu \equiv m\frac{dx^\mu}{d\tau}, \tag{2.8}$$

and rearranging indices, we have the following equation

$$m\frac{dp_\sigma}{d\tau} = \frac{1}{2}\left(\partial_\sigma g_{\mu\nu}\right) p^\mu p^\nu, \tag{2.9}$$

which is the geodesic equation expressed in terms of the 4-momentum. For a cyclic coordinate x^α, we have $\partial_\alpha g_{\mu\nu} = 0$, and therefore, Eq. (2.9) reduces to

$$m\frac{dp_\alpha}{d\tau} = 0 \Rightarrow p_\alpha = \text{constant}. \tag{2.10}$$

In addition, the coordinate basis vector ∂_α can be identified with a vector $K = \partial_\alpha$[3] such that $K_\sigma p^\sigma =$ constant [33]. This quantity is preserved along geodesic motion, hence, its directional derivative vanishes

$$\frac{dp_\sigma}{d\tau} = 0 \Rightarrow p^\rho \nabla_\rho (K_\sigma p^\sigma) = 0. \tag{2.11}$$

From the lhs of Eq. (2.11), one obtains an equivalent expression

$$p^\rho p^\sigma \nabla_{(\rho} K_{\sigma)} = 0, \tag{2.12}$$

which holds for vectors K satisfying $\nabla_{(\rho} K_{\sigma)} = 0$ and is known as *Killing's equation* [33].

Therefore, the symmetries in the metric satisfy the Killing's equation. Nevertheless, not all symmetries of the spacetime can be obtained from cyclic coordinates, in fact, we can find Killing vector fields that satisfy Eq. (2.12) and are not necessarily expressed as $K = \partial_\alpha$. Hence, the background spacetime (2.3) possesses two Killing vector fields as follows

$$\xi^\mu = (1, 0, 0, 0), \tag{2.13}$$

[3] In component notation this is $K^\mu = (\partial_\alpha)^\mu = \delta^\mu_\alpha$.

$$\psi^\mu = (0,0,0,1), \tag{2.14}$$

which are related to invariance of the metric under translations in the $t-$ and $\varphi-$coordinates. The aforementioned vector fields induce the following conserved quantities

$$E = \frac{\bar{E}}{m} = -\xi_\mu U^\mu = -g_{tt} U^t, \tag{2.15}$$

$$L = \frac{\bar{L}}{m} = \psi_\mu U^\mu = g_{\varphi\varphi} U^\varphi, \tag{2.16}$$

where E and L are the energy and angular momentum per unit mass, respectively. This yields the following expressions for two components of the 4-velocity

$$U^t = -\frac{E}{g_{tt}}, \tag{2.17}$$

$$U^\varphi = \frac{L}{g_{\varphi\varphi}}. \tag{2.18}$$

Due to the spherical symmetry of spacetime, we restrict the particle's motion to the equatorial plane $\theta = \pi/2$ without loss of generality, which implies that $U^\theta = 0$. Now, with the aid of Eqs. (2.17) and (2.18), Eq. (2.6) reduces to

$$-\frac{1}{2} g_{rr} g_{tt} (U^r)^2 - \frac{g_{tt}}{2} - \frac{g_{tt}}{2} \frac{L^2}{g_{\varphi\varphi}} = \frac{E^2}{2}, \tag{2.19}$$

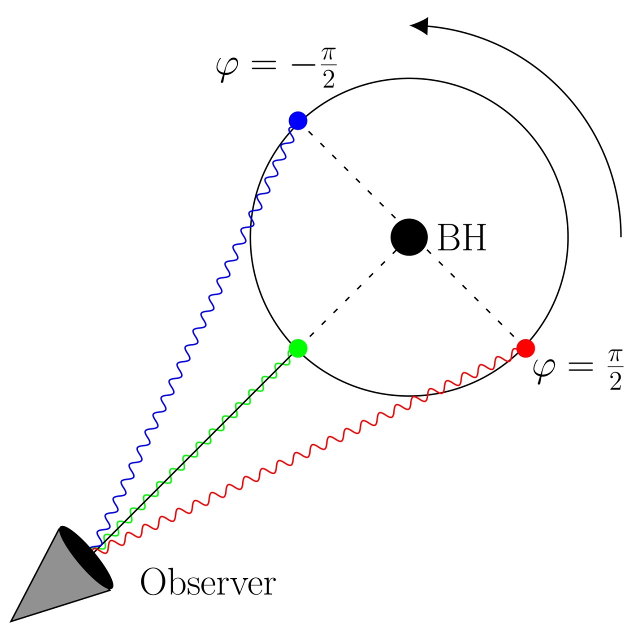

Figure 2.1: *Geometrical illustration of the model for the test particle (depicted as a red/blue/green dot in the diagram) - black hole system, with an observer located in the equatorial plane $\theta = \pi/2$. Here, we represent the frequency shift of light rays emitted by a massive probe particle orbiting the black hole in equatorial circular geodesic motion. The total redshift/blueshift becomes maximum at $\varphi = \pm\pi/2$.*

which has the energy conservation law structure such that the first term is the kinetic energy of the particle moving in an effective potential with the following form

$$V_{eff}=-\frac{g_{tt}}{2}\left(1+\frac{L^2}{g_{\varphi\varphi}}\right). \tag{2.20}$$

From Eq. (2.19), we define a function $V_r(r)$ related to the radial component of the 4-velocity as follows

$$g_{rr}(U^r)^2=-1-\frac{E^2}{g_{tt}}-\frac{L^2}{g_{\varphi\varphi}}\equiv V_r(r), \tag{2.21}$$

then, Eq. (2.19) can be expressed as

$$g_{rr}(U^r)^2-V_r(r)=0. \tag{2.22}$$

Taking into account the real astrophysical systems and spherical symmetry of the spacetime background, investigating circular equatorial motion is relevant. Besides, taking $\theta=\pi/2$ allows us to express some relations in a simpler way without loss of generality. Thus, we consider the massive test particles in equatorial circular orbits (see Figure 2.1) to describe the photon sources and their motion are governed by the following conditions

$$V_r(r)=-1-\frac{E^2}{g_{tt}}-\frac{L^2}{g_{\varphi\varphi}}=0, \tag{2.23}$$

$$V_r'(r)=\frac{E^2}{g_{tt}^2}g_{tt}'+\frac{L^2}{g_{\varphi\varphi}^2}g_{\varphi\varphi}'=0, \tag{2.24}$$

where the prime symbol denotes the derivative with respect to the radial coordinate r.

On the other hand, from Eq. (2.3), we have the following relations

$$g_{tt}=-f, \quad g_{rr}=g, \quad g_{\theta\theta}=h, \quad g_{\varphi\varphi}=h\,\sin^2\theta. \tag{2.25}$$

From conditions (2.23) and (2.24), along with the above mentioned relations, one can find E and L in terms of the metric functions f and h and their derivatives as below

$$E^2=h'\left(\frac{f^2}{fh'-hf'}\right), \tag{2.26}$$

$$L^2=h\left(\frac{E^2}{f}-1\right)=h\left[h'\left(\frac{f}{fh'-hf'}\right)-1\right]=f'\left(\frac{h^2}{fh'-hf'}\right). \tag{2.27}$$

Note that from Eq. (2.27), L possesses two signs referring to the rotation direction of test particles, namely, $+/-$ sign for counterclockwise/clockwise, from which we adopt the positive sign without loss of generality since we are dealing with a spherically symmetric spacetime.

Now, with the aid of these relations, $t-$ and $\varphi-$ components of the 4-velocity given in Eqs. (2.17) and (2.18), can be expressed as follows

$$U_e^t=-\frac{E}{g_{tt}}=\left.\sqrt{\frac{h'}{fh'-hf'}}\right|_{r_e}, \tag{2.28}$$

$$U_e^\varphi=\frac{L}{g_{\varphi\varphi}}=\left.\sqrt{\frac{f'}{fh'-hf'}}\right|_{r_e}, \tag{2.29}$$

in terms of the metric functions and their derivatives that characterize the black hole parameters and subscript e refers to the emitter radius r_e.

For stability of the circular orbits, the second derivative of $V_r(r)$ is required to satisfy the following condition

$$V_r''(r)=-\frac{2E^2}{g_{tt}^3}\left(g_{tt}'\right)^2+\frac{E^2}{g_{tt}^2}g_{tt}''-\frac{2L^2}{g_{\varphi\varphi}^3}\left(g_{\varphi\varphi}'\right)^2+\frac{L^2}{g_{\varphi\varphi}^2}g_{\varphi\varphi}''\leq 0, \tag{2.30}$$

where the equality indicates the innermost stable circular orbit (ISCO) and characterizes the inner edge of the accretion disk. Now, by using the relations (2.25) it is possible to find an explicit expression for $V_r''(r)$ in terms of the metric functions f and h and their derivatives with the aid of Eqs. (2.26) and (2.27), which reads

$$V_r''(r) = \frac{1}{hf' - fh'} \left\{ h' \left[f'' - \frac{2}{f} (f')^2 \right] + f' \left[\frac{2}{h} (h')^2 - h'' \right] \right\}. \tag{2.31}$$

2.2 Massless particles

In the case of massless particles, which follow null geodesics, the equation of motion (2.5) reads [4]

$$g_{\mu\nu} k^\mu k^\nu = g_{tt}(k^t)^2 + g_{rr}(k^r)^2 + g_{\theta\theta}(k^\theta)^2 + g_{\varphi\varphi}(k^\varphi)^2 = 0, \tag{2.32}$$

where $k^\mu = (k^t, k^r, k^\theta, k^\varphi)$ is the 4-wave vector of the photons.

These photons move in the black hole spacetime described by the metric (2.3), which depends on the explicit form of the functions f, g, and h, and outside the event horizon. By considering the motion of photons on the equatorial plane, the component k^θ of the 4-wave vector vanishes, hence Eq. (2.32) reduces to

$$g_{tt}(k^t)^2 + g_{rr}(k^r)^2 + g_{\varphi\varphi}(k^\varphi)^2 = 0. \tag{2.33}$$

Due to the symmetries present in the spherically symmetric spacetime, we have the Killing vector fields ξ^μ and ψ^μ from Eqs. (2.13) and (2.14), respectively. Therefore, the following conserved quantities also hold for photon motion

$$E_\gamma = -\xi_\mu k^\mu = -g_{tt} k^t, \tag{2.34}$$

$$L_\gamma = \psi_\mu k^\mu = g_{\varphi\varphi} k^\varphi. \tag{2.35}$$

Hence, it is possible to express $t-$ and φ-components of the 4-wave vector in terms of the energy and angular momentum of photons as follows

$$k^t = -\frac{E_\gamma}{g_{tt}}, \tag{2.36}$$

$$k^\varphi = \frac{L_\gamma}{g_{\varphi\varphi}}. \tag{2.37}$$

Now, by substituting these relations into the equation of motion (2.33), we have

$$g_{rr}(k^r)^2 + \frac{E_\gamma^2}{g_{tt}} + \frac{L_\gamma^2}{g_{\varphi\varphi}} = 0. \tag{2.38}$$

Note that for the points where the radial component of the 4-wave vector k^r vanishes (which are the diametrically opposite points whose joint line is perpendicular to the line of sight), Eq. (2.38) simplifies in the following way

$$\frac{E_\gamma^2}{g_{tt}} + \frac{L_\gamma^2}{g_{\varphi\varphi}} = 0, \tag{2.39}$$

then

$$\frac{1}{g_{tt}} + \frac{L_\gamma^2}{E_\gamma^2 g_{\varphi\varphi}} = \frac{1}{g_{tt}} + b_\gamma^2 \frac{1}{g_{\varphi\varphi}} = 0, \tag{2.40}$$

where we defined the *deflection of light parameter* as follows[5]

$$b_\gamma \equiv \frac{L_\gamma}{E_\gamma}. \tag{2.41}$$

[4] As stated before, in this case we cannot use the proper time τ, instead, one uses the affine parameter λ.

[5] For more information about the deflection parameter, see [1].

Now, from Eq. (2.40) one can obtain an expression for the deflection parameter in terms of the properties of the spacetime as follows

$$b_{\gamma\pm} = \pm\sqrt{-\frac{g_{\varphi\varphi}}{g_{tt}}}, \tag{2.42}$$

and by using $g_{tt} = -f$ and $g_{\varphi\varphi} = h$, we have

$$b_{\gamma\pm} = \pm\sqrt{\frac{h}{f}}. \tag{2.43}$$

This relation shows the deflection of light sources due to curvature of the spacetime, when they are located on either side of the black hole at the midline characterized by $\pm$ sign.

Chapter 3

The frequency shift of photons emitted by geodesic massive particles in a general spherically symmetric spacetime

In the study of the cosmos, observational evidence is of great relevance due to its importance in testing theoretical proposals. In the case of black holes, they produce a very strong gravitational field from which even light cannot escape. However, information on black hole parameters can be obtained from orbiting objects in its vicinity (such as stars or water vapor clouds). The information of the background spacetime of the black hole is encoded in light emitted from these objects, and due to gravitational curvature and orbital motion, photons detected on the Earth experience frequency shift that can be quantified using methods such as spectroscopy.

In this regard, the general relativistic method introduced in [13–15] provides a way to express the frequency shift of photons in terms of the free parameters of spacetime and the orbital parameters of test particles orbiting the black hole by taking into account the 4-velocity of the test particles and the 4-wave vector of the emitted photons for axially symmetric backgrounds, namely, the Kerr and Kerr de-Sitter spacetimes, and some analysis for Schwarzschild and Scharzschild de-Sitter spacetimes. This allows us to estimate the black hole parameters by measuring the shift in the frequency of photons and solving an inverse problem to obtain the black hole parameters in terms of observable quantities.

Here, we present an overview of the method developed in [13–15] and we extend it to a general spherically symmetric background with the help of the results of the previous chapter. To this end, we first consider the expression for the energy of a particle with 4-momentum p^μ measured by an observer with 4-velocity U^μ [33]

$$E = -p^\mu U_\mu, \tag{3.1}$$

and in the case of photons, its 4-momentum is related to the 4-wave vector by means of the following expression

$$p_\mu = \hbar k_\mu, \tag{3.2}$$

where $\hbar$ is the reduced Planck's constant. Therefore, the energy of a photon measured by an observer with 4-velocity U^μ reads

$$E_\gamma = -\hbar\, k_\mu U^\mu. \tag{3.3}$$

From the Einstein-Planck relation $E_\gamma = \hbar\omega$, alongside Eq. (3.3) yields the following relation[1]

$$\omega_p = -k_\mu U^\mu\big|_p\,, \tag{3.4}$$

where the index p refers to either the point of emission $x_e^\mu = (x^t, x^r, x^\theta, x^\varphi)|_e$ or detection $x_d^\mu = (x^t, x^r, x^\theta, x^\varphi)|_d$ of the photon.

Hence, the frequency shift of photons from emission till detection is given by

$$1 + z_{_{BH}} = \frac{\omega_e}{\omega_d}, \tag{3.5}$$

which for static and spherically symmetric backgrounds of the form (2.3) takes the general form [13–15]

$$1 + z_{_{BH}} = \frac{\left(E_\gamma U^t - L_\gamma U^\varphi - g_{rr}k^r U^r - g_{\theta\theta}k^\theta U^\theta\right)\big|_e}{\left(E_\gamma U^t - L_\gamma U^\varphi - g_{rr}k^r U^r - g_{\theta\theta}k^\theta U^\theta\right)\big|_d}. \tag{3.6}$$

In addition, if the motion of massive test particles is restricted to the equatorial plane and circular orbits, respectively, implying that $U^\theta = 0$ and $U^r = 0$, the frequency shift formula (3.6) reduces to

$$1 + z_{_{BH}} = \frac{\left(E_\gamma U^t - L_\gamma U^\varphi\right)\big|_e}{\left(E_\gamma U^t - L_\gamma U^\varphi\right)\big|_d}. \tag{3.7}$$

Furthermore, by considering the observer at a very large distance from the black hole (ideally at spatial infinity $r_d \to \infty$), its 4-velocity is given by $U_d^\mu = (1, 0, 0, 0)$, and therefore the frequency shift simplifies to

$$1 + z_{_{BH_{1,2}}} = U_e^t - b_{\gamma\mp} U_e^\varphi, \tag{3.8}$$

where we used the light deflection parameter defined in Eq. (2.41) and the index 1 (2) refers to $-$ $(+)$ sign of $b_{\gamma\pm}$. One may note that the angular momentum L presented in Eq. (3.7) also possesses $\pm$ signs according to Eq. (2.27) which amounts to the rotation direction of massive particles ($+/-$ for counter-clockwise/clockwise). However, due to the spherical symmetry of the background, we choose the plus sign without loss of generality.

Finally, by substituting Eqs. (2.28), (2.29) and (2.43) into Eq. (3.8), one obtains the following general expression

$$1 + z_{_{BH_{1,2}}} = \sqrt{\frac{\frac{\partial h}{\partial r}}{f\frac{\partial h}{\partial r} - h\frac{\partial f}{\partial r}}} \pm \sqrt{\frac{h}{f}\left(\frac{\frac{\partial f}{\partial r}}{f\frac{\partial h}{\partial r} - h\frac{\partial f}{\partial r}}\right)} = \frac{\sqrt{\frac{\partial h}{\partial r}} \pm \sqrt{\frac{h}{f}\frac{\partial f}{\partial r}}}{\sqrt{f\frac{\partial h}{\partial r} - h\frac{\partial f}{\partial r}}}. \tag{3.9}$$

for the shift in the frequency of photon sources circularly orbiting a general spherically symmetric black hole spacetime of the form (2.3). In this relation, $z_{_{BH_1}}/z_{_{BH_2}}$ corresponds to the $+/-$ sign that represents the redshift/blueshift at the midline and on either side of the line of sight. It is important to remark here that the aforementioned expression is the total frequency shift where the first term corresponds to the gravitational frequency shift and the second term is the kinematic frequency shift such that

$$1 + z_{_{BH_{1,2}}} = 1 + z_g + z_{kin_\pm}. \tag{3.10}$$

On the other hand, as discussed in previous chapters, curvature singularities have been a controversial prediction from GR, and many attempts have been made to get rid of this issue. In this direction, conformally invariant gravitational theories are one of the most successful ways to avoid these essential singularities. As a concrete example of the application of this general relativistic approach, we shall study a nonsingular black hole conformally related to the Schwarzschild black hole, and compare its frequency shift to the standard Schwarzschild black hole frequency shift.

[1] Note that unlike radial velocities used in Newtonian gravity, ω_p is a general relativistic invariant, *i.e.* it does not depend on the coordinate system [14].

Chapter 4

The frequency shift of photons emitted by test particles orbiting nonsingular black holes in conformal gravity

In order to show the application of the results obtained in the previous chapters regarding the frequency shift of test particles revolving spherically symmetric spacetimes, we take into account the nonsingular black holes (1.13) in conformal gravity as a special example. As we discussed in chapter (1), it is possible to remove the black hole singularity of the Schwarzschild spacetime by means of a suitable conformal transformation. In order to remove the spacetime singularity of the Schwarzschild black hole, we consider the conformal factor (1.12). Note that for the case of the Schwarzschild black hole, the background spacetime depends only on the mass parameter M, and after the conformal transformation, the new nonsingular spacetime (1.13) depends on the three parameters l, N, and M. Then, we can consider massive geodesic test particles circularly orbiting the conformal black hole described by Eq. (1.13) and apply all the formalism developed in the previous chapters.

First, we note that it is possible to restrict the motion of orbiting particles to the equatorial plane ($\theta = \pi/2$) due to the spherical symmetry of the spacetime, hence the metric component $\hat{g}_{\varphi\varphi}$ (1.17) reduces to

$$\hat{g}_{\varphi\varphi} = h = \left(1 - \frac{l^2}{r^2}\right)^{2N} r^2. \tag{4.1}$$

Now, we express Eq. (2.31) in terms of the free parameters of the spacetime with the aid of the metric functions (1.14) and (4.1) in order to obtain r_{ISCO}. To this end, it is necessary to compute the first and second derivatives of the metric functions f and h with respect to the radial coordinate r

$$\frac{\partial f}{\partial r} = 2\left[\frac{2Nl^2(r-2M) + M(r^2 - l^2)}{r^2(r^2 - l^2)}\right]\left(1 - \frac{l^2}{r^2}\right)^{2N}, \tag{4.2}$$

$$\frac{\partial h}{\partial r} = \left(1 - \frac{l^2}{r^2}\right)^{2N} 2r\left[\frac{2Nl^2 + r^2 - l^2}{r^2 - l^2}\right], \tag{4.3}$$

$$\begin{aligned}\frac{\partial^2 f}{\partial r^2} = \left(1 - \frac{l^2}{r^2}\right)^{2N} \frac{4}{r^3(r^2 - l^2)^2}[&-Mr^4 - 3Nl^2r^3 + (5N+1)2Ml^2r^2 + (4N+1)Nl^4r \\ &- (6N + 8N^2 + 1)Ml^4],\end{aligned} \tag{4.4}$$

$$\frac{\partial^2 h}{\partial r^2} = \left(1 - \frac{l^2}{r^2}\right)^{2N} \frac{2}{(r^2 - l^2)^2}[r^4 + (N-1)2l^2r^2 + 2l^4(4N^2 - 3N + 1)]. \tag{4.5}$$

For the sake of clarity, we present the computation of the terms and factors involved in Eq. (2.31). First, we have the following expressions

$$\frac{2}{f}\left(\frac{\partial f}{\partial r}\right)^2=\left(1-\frac{l^2}{r^2}\right)^{2N}\frac{8[2Nl^2(r-2M)+M(r^2-l^2)]^2}{(r-2M)\,r^3(r^2-l^2)^2}, \tag{4.6}$$

$$\frac{2}{h}\left(\frac{\partial h}{\partial r}\right)^2=\left(1-\frac{l^2}{r^2}\right)^{2N}\frac{8(2Nl^2r+r^3-l^2r)^2}{r^2(r^2-l^2)^2}, \tag{4.7}$$

therefore, the first term in brackets in Eq. (2.31) reads

$$\frac{\partial^2 f}{\partial r^2}-\frac{2}{f}\left(\frac{\partial f}{\partial r}\right)^2=\frac{4\left(1-\frac{l^2}{r^2}\right)^{2N}}{r^3(r^2-l^2)^2(r-2M)}\left[-Mr^5-3Nl^2r^4+(8MN+2M)l^2r^3\right.$$
$$\left.+(Nl^4-4N^2l^4-4M^2Nl^2)r^2+(16MN^2-M)l^4r-(4M^2N+16M^2N^2)l^4\right]. \tag{4.8}$$

In addition, this term was multiplied by $\frac{dh}{dr}$ in the r_{ISCO} equation (2.31), and thus with the aid of Eq. (4.3), it can be expressed as follows

$$\frac{\partial h}{\partial r}\left[\frac{\partial^2 f}{\partial r^2}-\frac{2}{f}\left(\frac{\partial f}{\partial r}\right)^2\right]=4\left(1-\frac{l^2}{r^2}\right)^{4N}\left(\frac{4Nl^2r+2r^3-2l^2r}{r^3(r^2-l^2)^3(r-2M)}\right)(-Mr^5-3Nl^2r^4$$
$$+(8MN+2M)l^2r^3+(Nl^4-4N^2l^4-4M^2Nl^2)r^2+(16MN^2-M)l^4r-(4M^2N+16M^2N^2)l^4)$$
$$=\frac{4\left(1-\frac{l^2}{r^2}\right)^{4N}}{r^2(r^2-l^2)^3(r-2M)}\left[-2Mr^7-6Nl^2r^6+(12N+6)Ml^2r^5+(8Nl^4-20N^2l^4-8M^2Nl^2)r^4\right.$$
$$+(64N^2-6-8N)Ml^4r^3+(12N^2l^6-16N^3l^6-48M^2N^2l^4-2Nl^6)r^2$$
$$\left.+(2-32N^2+64N^3-4N)Ml^6r+(16N^2-64N^3+8N)M^2l^6\right]. \tag{4.9}$$

Similarly, for the second term of the r_{ISCO} equation, we have

$$\frac{\partial f}{\partial r}\left[\frac{2}{h}\left(\frac{\partial h}{\partial r}\right)^2-\frac{\partial^2 h}{\partial r^2}\right]=\frac{4\left(1-\frac{l^2}{r^2}\right)^{4N}}{r^2(r^2-l^2)^3}\left[3Mr^6+6Nl^2r^5+(2N-9)Ml^2r^4+(28N^2-12N)l^4r^3\right.$$
$$\left.+(9-48N^2)Ml^4r^2+(16N^3-20N^2+6N)l^6r+(32N^2-2N-3-32N^3)Ml^6r\right]$$
$$=\frac{4\left(1-\frac{l^2}{r^2}\right)^{4N}}{r^2(r^2-l^2)^3(r-2M)}\left[3Mr^7+6(Nl^2-M^2)r^6-(10N+9)Ml^2r^5\right.$$
$$+(28N^2l^4-12Nl^4-4NM^2l^2+18M^2l^2)r^4+(9+24N-104N^2)Ml^4r^3$$
$$+(16N^3l^6-20N^2l^6+6Nl^6-18M^2l^4+96M^2N^2l^4)r^2+(72N^2-14N-64N^3-3)Ml^6r$$
$$\left.+(4N-64N^2+6+64N^3)M^2l^6\right]. \tag{4.10}$$

Therefore, by considering the relations (4.9) and (4.10), the numerator of Eq. (2.31) reads

$$\frac{\partial h}{\partial r}\left[\frac{\partial^2 f}{\partial r^2}-\frac{2}{f}\left(\frac{\partial f}{\partial r}\right)^2\right]+\frac{\partial f}{\partial r}\left[\frac{2}{h}\left(\frac{\partial h}{\partial r}\right)^2-\frac{\partial^2 h}{\partial r^2}\right]=\frac{4\left(1-\frac{l^2}{r^2}\right)^{4N}}{r^2(r^2-l^2)^3(r-2M)}\left[Mr^7-6M^2r^6\right.$$
$$+(2N-3)Ml^2r^5+(8N^2l^4-4Nl^4+18M^2l^2-12NM^2l^2)r^4+(16N-40N^2+3)Ml^4r^3$$
$$+(4Nl^6-8N^2l^6+48M^2N^2l^4-18M^2l^4)r^2$$
$$\left.+(40N^2-18N-6)Ml^6r+(12N-48N^2+6)M^2l^6\right], \tag{4.11}$$

and the denominator in the r_{ISCO} equation (2.31) is given by

$$f\frac{\partial h}{\partial r} - h\frac{\partial f}{\partial r} = 2\left(1 - \frac{l^2}{r^2}\right)^{4N}(r - 3M). \tag{4.12}$$

Then, the expression for $V_r''(r)$ in terms of the free parameters of the conformal gravity reads

$$\begin{aligned} V_r''(r) &= \frac{1}{f\frac{\partial h}{\partial r} - h\frac{\partial f}{\partial r}}\left\{\frac{\partial h}{\partial r}\left[\frac{\partial^2 f}{\partial r^2} - \frac{2}{f}\left(\frac{\partial f}{\partial r}\right)^2\right] + \frac{\partial f}{\partial r}\left[\frac{2}{h}\left(\frac{\partial h}{\partial r}\right)^2 - \frac{\partial^2 h}{\partial r^2}\right]\right\} \\ &= \frac{1}{2(r-3M)(r-2M)r^2(r^2-l^2)^2}[Mr^5 - 6M^2r^4 + 2Ml^2(N-1)r^3 \\ &+ 4l^2((2N-1)Nl^2 - 3M^2(N-1))r^2 + (1+18N-40N^2)Ml^4r + (8N^2-2N-1)6M^2l^4]. \end{aligned} \tag{4.13}$$

Hence, to find the r_{ISCO} by solving $V_r''(r) = 0$, one must obtain the roots of the following 5th-order polynomial

$$\begin{aligned} &r^5 - 6Mr^4 + 2l^2(N-1)r^3 + 4M^{-1}l^2((2N-1)Nl^2 - 3M^2(N-1))r^2 \\ &+ (1+18N-40N^2)l^4r + (8N^2-2N-1)6Ml^4 = 0, \end{aligned} \tag{4.14}$$

and we have stable orbits for the radii $r \geq r_{ISCO}$. It is important to remark that this equation cannot be solved analytically and we shall use its numerical solutions in our future analyses. Nonetheless, the black curves in Figs. 4.1-4.2 show the dependency of r_{ISCO} on the free parameters N and l of the theory. From these figures, we see that for nonvanishing values of the free parameters, $r_{ISCO}^{(CG)}$ in conformal gravity is always less than $r_{ISCO}^{(Schw)} = 6$ for the Schwarzschild black hole case, $r_{ISCO}^{(CG)} < r_{ISCO}^{(Schw)}$. It is worth mentioning that although it is possible to have circular orbits for $r_e < r_{ISCO}$, these orbits are not stable. Hence, the region of interests corresponds to values of r greater than r_{ISCO} for which bounded orbits are stable.

A numerical investigation of the solutions to Eq. (4.14) in black hole mass unit for $N = 1, 2$ and $0 \leq l \leq 1$ indicates that there is only one positive definite root larger that the photon sphere radius r_{ph} and the rest of the roots are either imaginary/complex-valued or smaller than r_{ph} [r_{ph} can be obtained through the condition $(g'_{tt}g_{\varphi\varphi})_{r=r_{ph}} = (g_{tt}g'_{\varphi\varphi})_{r=r_{ph}}$ and this constraint is deduced from Eq. (2.38) by considering the condition $k^r = 0$]. Hence, the positive definite root of Eq. (4.14) satisfying $r_{ISCO} > r_{ph}$ indicates the ISCO radius.

In addition, given the expressions for the metric functions f, g, h and their derivatives, it is possible to compute the explicit expressions (2.28)-(2.29) for U_e^t and U_e^φ in terms of the parameters N, l, M and the radius of the emitter r_e

$$U_e^t = \sqrt{\frac{2Nl^2r_e + r_e(r_e^2 - l^2)}{(r_e - 3M)(r_e^2 - l^2)}\left(1 - \frac{l^2}{r_e^2}\right)^{-2N}}, \tag{4.15}$$

$$U_e^\varphi = \sqrt{\frac{2Nl^2r_e - 4MNl^2 + M(r_e^2 - l^2)}{(r_e - 3M)(r_e^2 - l^2)}\left(1 - \frac{l^2}{r_e^2}\right)^{-2N}}, \tag{4.16}$$

where for large emitter radius, they reduce to

$$\lim_{r_e \to \infty} U_e^t = 1, \tag{4.17}$$

$$\lim_{r_e \to \infty} U_e^\varphi = 0. \tag{4.18}$$

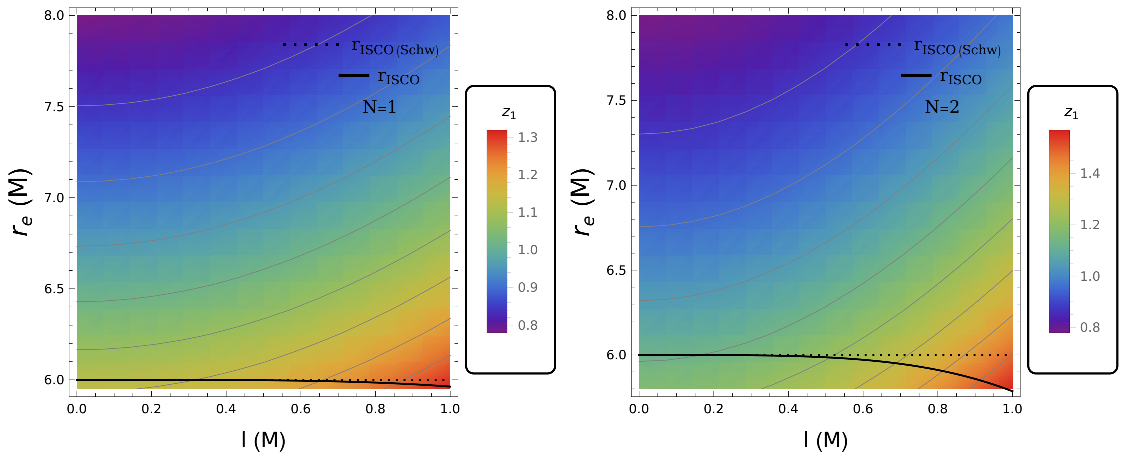

Figure 4.1: *The redshift in the $r_e - l$ plane for M=1. The gray curves stand for constant values of z_1 and the black curves denote $r_e = r_{ISCO}$.*

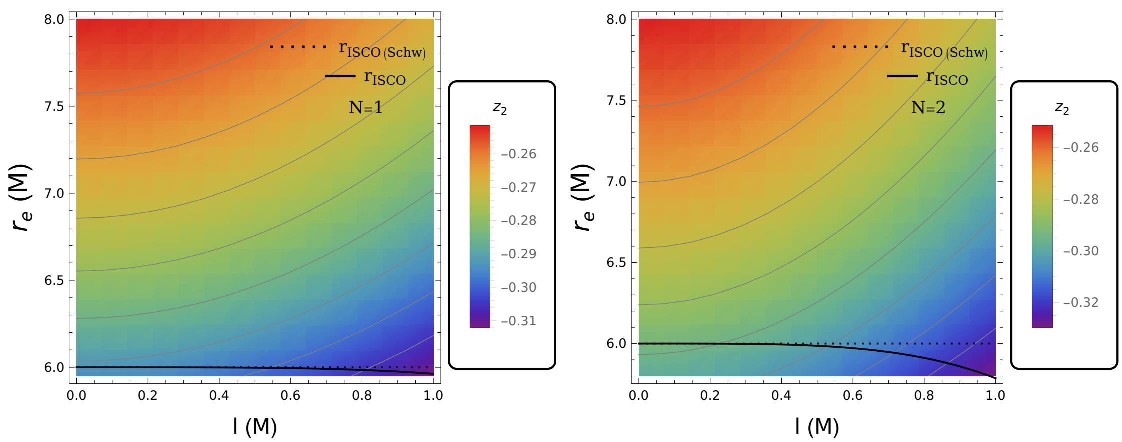

Figure 4.2: *The blueshift in the $r_e - l$ plane for M=1. The gray curves represent the constant levels of the blueshift and the black curves stand for $r_e = r_{ISCO}$.*

On the other hand, by substituting Eqs. (1.14) and (4.1)-(4.3) into the general relation (3.9), we are able to express the total observational frequency shift in the conformal gravity spacetime in terms of the parameters l, N, M, and the radius of the emitter r_e as follows

$$1 + z_{_{1,2}} = \frac{\sqrt{r_e(2Nl^2 + r_e^2 - l^2)(r_e - 2M)} \pm \sqrt{r_e[Mr_e^2 + 2Nl^2 r_e - Ml^2(4N+1)]}}{\sqrt{\left(1 - \frac{l^2}{r_e^2}\right)^{2N} (r_e - 3M)(r_e - 2M)(r_e^2 - l^2)}}, \tag{4.19}$$

where z_1/z_2 corresponds to redshift/blueshift. Besides, from Eq. (4.19) one can identify

$$1 + z_g = \frac{\sqrt{r_e(2Nl^2 + r_e^2 - l^2)}}{\sqrt{\left(1 - \frac{l^2}{r_e^2}\right)^{2N} (r_e - 3M)(r_e^2 - l^2)}}, \tag{4.20}$$

and

$$z_{kin_\pm} = \pm \frac{\sqrt{r_e[Mr_e^2 + 2Nl^2 r_e - Ml^2(4N+1)]}}{\sqrt{\left(1 - \frac{l^2}{r_e^2}\right)^{2N} (r_e - 3M)(r_e - 2M)(r_e^2 - l^2)}}, \tag{4.21}$$

as, respectively, the gravitational frequency shift and kinematic frequency shift satisfying $z_{_{1,2}} = z_g + z_{kin_\pm}$. Note that these formulas reduce to the Schwarzschild case [19] for either $N = 0$ or $l = 0$, as it should be. In addition, since $z_{_{1,2}}$ are observable quantities, the aforementioned relations can be employed together with the real astrophysical data in order to estimate (or constraint) the nonsingular black hole parameters N and l appearing in this model of conformal gravity.

Note that the length scale parameter l has been constrained with the help of x-ray observational data of the supermassive black hole 1H0707-495 to be $l \leq 0.6$ for $N = 2$ [34] and $l \leq 0.225$ for $N = 1$ [35]. Therefore, we concentrate our attention on the restricted values $N = 1, 2$ and $0 \leq l \leq 1$ for the free parameters of the conformal gravity in our analysis. Figs. 4.1-4.2 illustrate the density plots of the redshift and blueshift in the $r_e - l$ parameter space for $N = 1, 2$. As one can see from these figures, r_e and l have opposite effects on the redshift/blueshift and as r_e (l) increases, the shift in frequency decreases (increases). Therefore, it is expected that these parameters balance the frequency shift at some points, denoted by the continuous gray curves in Figs. 4.1 and 4.2, which represent constant level sets for $z_{_{1,2}}$.

In addition, from Fig. 4.3, we find that the redshift, blueshift, and gravitational redshift increase when the free parameter N increases. Moreover, this figure shows that as the parameter N takes greater values, the frequency shift curves increase faster as a function of l since N appears as an exponent in the conformal factor Ω^2. As the free parameters take higher values, $z_{_{1,2}}$ significantly deviates from the Schwarzschild redshift/blueshift depicted in Fig. 4.3 as $N = 0$. It is worth mentioning that although z_g is positive and increases as the free parameters increase (see the right panel of Fig. 4.3), z_2 is still negative and acquires lower values for nonvanishing N and l since $z_{kin_\pm}$-term is dominant (see the middle panel of Fig. 4.3).

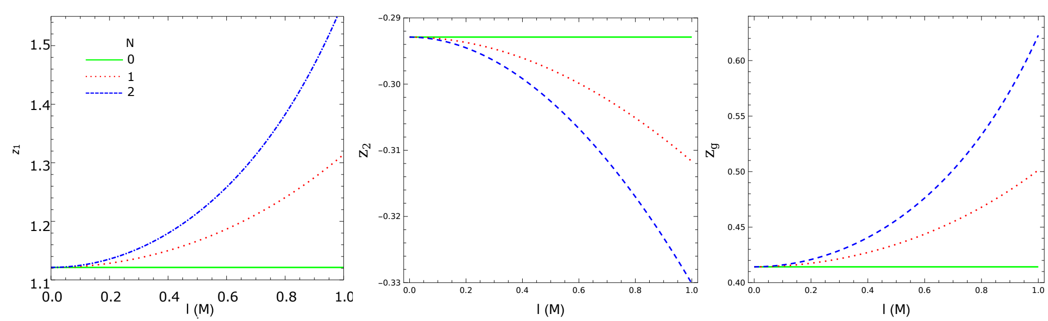

Figure 4.3: *The redshift z_1 (left), blueshift z_2 (middle) and gravitational redshift z_g (right) versus the length scale l for various values of N and $M = 1$. The emitter is orbiting circularly at $r_e = r_{ISCO}$ and the continuous green curves refer to the frequency shift in the Schwarzschild spacetime where $N = 0$.*

Furthermore, by defining $R = 1 + z_1$ and $B = 1 + z_2$, one can readily verify

$$RB = \frac{1}{\Omega^2(r_e)\left(1 - \frac{2M}{r_e}\right)}, \tag{4.22}$$

which leads to an expression for the mass of the nonsingular black hole in terms of the observable frequency shifts z_1 and z_2 as well as the free parameters l and N of the conformal gravity theory in the following way

$$M = \frac{RB - \left(\frac{r_e^2}{r_e^2 - l^2}\right)^{2N}}{2RB} r_e = \frac{(1+z_1)(1+z_2) - \left(\frac{r_e^2}{r_e^2 - l^2}\right)^{2N}}{2(1+z_1)(1+z_2)} r_e, \tag{4.23}$$

which reduces to the Schwarzschild black hole mass formula for either vanishing N or l.

In addition, it is worth noting that by taking into account the frequency shift formulas (4.19) and the conformal factor (1.12) for the special case $N = 1$, one can show that

$$\mathcal{X} \equiv RB = \frac{r_e}{(r_e - 2M)\Omega^2(r_e)}, \tag{4.24}$$

$$\mathcal{Y} \equiv (R+B)^2 = \frac{4[2-\Omega(r_e)]r_e}{(r_e - 3M)\Omega^3(r_e)}. \tag{4.25}$$

In order to express the free parameters M and l in terms of observable quantities, we make use of expressions (4.24) and (4.25) to obtain the following equation for Ω

$$\Omega^3 - \left(\frac{8}{\mathcal{Y}} + \frac{3}{\mathcal{X}}\right)\Omega + \frac{16}{\mathcal{Y}} = 0, \tag{4.26}$$

which is a cubic equation of the form $x^3 + px + q = 0$, where

$$p = -\left(\frac{8}{\mathcal{Y}} + \frac{3}{\mathcal{X}}\right), \tag{4.27}$$

$$q = \frac{16}{\mathcal{Y}}, \tag{4.28}$$

and has the following solutions

$$\Omega_1 = \sqrt[3]{A_+} + \sqrt[3]{A_-}, \qquad \Omega_2 = \zeta_1\sqrt[3]{A_+} + \zeta_2\sqrt[3]{A_-}, \qquad \Omega_3 = \zeta_2\sqrt[3]{A_+} + \zeta_1\sqrt[3]{A_-}, \tag{4.29}$$

where $\zeta_1 = \cos(2\pi/3) + i\sin(2\pi/3)$ and $\zeta_2 = \cos(4\pi/3) + i\sin(4\pi/3)$ are the complex cube roots of unity in polar form, and $A_\pm$ is given by

$$A_\pm = -\frac{q}{2} \pm \sqrt{D}, \tag{4.30}$$

where $D = (27q^2 + 4p^3)/108$ is the discriminant and has the following explicit form in terms of $\mathcal{X}$ and $\mathcal{Y}$

$$D = \frac{64(27\mathcal{Y} - 8)\mathcal{X}^3 - 576\mathcal{X}^2\mathcal{Y} - 216\mathcal{X}\mathcal{Y}^2 - 27\mathcal{Y}^3}{27\mathcal{X}^3\mathcal{Y}^3}. \tag{4.31}$$

Now, since the variables $\mathcal{X}$ and $\mathcal{Y}$ depend on the observable data of redshift and blueshift of photons, the typical values of z_1 and z_2 are such that the discriminant (4.31) is negative, and this yields three real roots for Eq. (4.26) [36]. Thus, given a negative discriminant, the parameter $A_\pm$ is a complex number, hence the solutions (4.29) involve working with the cube root of a complex number which can be addressed by computing its module

$$|A_\pm| = \left(-\frac{p}{3}\right)^{\frac{3}{2}}, \tag{4.32}$$

and its argument can be determined by the arccosine as follows

$$\sigma = \arccos\frac{q\sqrt{27}}{2p\sqrt{-p}}. \tag{4.33}$$

Therefore, the cube root of $A_\pm$ reads

$$A_\pm = \sqrt{-\frac{p}{3}}\left(\cos\frac{\sigma}{3} \pm i\sin\frac{\sigma}{3}\right), \tag{4.34}$$

and by using the solutions (4.29), one obtains the following expressions

$$\Omega_1 = 2\sqrt{-\frac{p}{3}}\cos\frac{\sigma}{3}, \tag{4.35}$$

$$\Omega_2 = -2\sqrt{-\frac{p}{3}}\cos\,\frac{\pi-\sigma}{3}, \tag{4.36}$$

$$\Omega_3 = -2\sqrt{-\frac{p}{3}}\cos\,\frac{\pi+\sigma}{3}. \tag{4.37}$$

We find that among the three solutions (4.35)-(4.37), only the solutions Ω_1 and Ω_3 give the correct values for the mass and the parameter l in the regions $\frac{M}{r_e} \geq \frac{1}{6}$ and $\frac{M}{r_e} < \frac{1}{6}$, respectively. Thus, as the final step, from Eq. (4.24) the mass of the black hole reads

$$M = \left(1 - \frac{1}{\mathcal{X}\Omega_{1,3}^2}\right)\frac{r_e}{2}, \tag{4.38}$$

and by substituting Eqs. (4.35) and (4.37) in this relation, we obtain an analytical expression for the black hole mass only in terms of the observational redshift/blueshift and orbital parameter of the emitter as follows

$$M = \begin{cases} \frac{r_e}{2}\left(1 - \frac{3\mathcal{Y}\sec^2\left(\frac{\pi+\sigma}{3}\right)}{4(8\mathcal{X}+3\mathcal{Y})}\right) & \text{for } \frac{M}{r_e} < \frac{1}{6}, \\ \frac{r_e}{2}\left(1 - \frac{3\mathcal{Y}\sec^2\left(\frac{\sigma}{3}\right)}{4(8\mathcal{X}+3\mathcal{Y})}\right) & \text{for } \frac{M}{r_e} \geq \frac{1}{6}. \end{cases} \tag{4.39}$$

Similarly, by using the relation $\Omega(r_e) = 1 - \frac{l^2}{r_e^2}$, we obtain the following explicit expression for the length parameter l

$$l = \begin{cases} r_e\left(1 + \frac{2\sqrt{8\mathcal{X}+3\mathcal{Y}}\cos\left(\frac{\pi+\sigma}{3}\right)}{\sqrt{3\mathcal{X}\mathcal{Y}}}\right)^{\frac{1}{2}} & \text{for } \frac{M}{r_e} < \frac{1}{6}, \\ r_e\left(1 - \frac{2\sqrt{8\mathcal{X}+3\mathcal{Y}}\cos\left(\frac{\sigma}{3}\right)}{\sqrt{3\mathcal{X}\mathcal{Y}}}\right)^{\frac{1}{2}} & \text{for } \frac{M}{r_e} \geq \frac{1}{6}. \end{cases} \tag{4.40}$$

where the parameter σ in terms of the variables $\mathcal{X}$ and $\mathcal{Y}$ reads

$$\sigma = \arccos\left(-\frac{24\mathcal{X}^{\frac{3}{2}}\mathcal{Y}^{\frac{1}{2}}\sqrt{3}}{(8\mathcal{X}+3\mathcal{Y})^{\frac{3}{2}}}\right). \tag{4.41}$$

Chapter 5

Conclusion

In this thesis, we have extended a general relativistic method [13–15] for measuring the black hole parameters to general spherically symmetric spacetimes by considering massive geodesic particles circularly orbiting a static black hole. Then, we have analytically obtained a general formula for the observational frequency shift of photons emitted by the test particles in terms of the metric functions and their derivatives that characterize the black hole parameters.

In addition, we have studied a special case by applying the former results to a nonsingular black hole conformally related to the Schwarzschild solutions as a concrete example of this general relativistic approach. Furthermore, we have investigated the effects of the free parameters of the conformal gravity theory on the observational redshift and compared results with those of the standard Schwarzschild black hole. Specifically, we have seen that for nonvanishing values of the free parameters N and l of the conformal gravity theory, the total observational redshift/blueshift increases. It was also found that an increase in either N or l parameter yields a decrease in r_{ISCO}, nevertheless, for the constrained values of $0 \leq l \leq 1$ and $N = 1, 2$, the difference between $r_{ISCO}^{(CG)}$ and $r_{ISCO}^{(Schw)}$ was negligible. Besides, for the case $N = 1$ and with the aid of the expressions obtained for redshift/blueshift, we have expressed the nonsingular black hole mass M and length scale parameter l of the conformal gravity theory in terms of the observational redshift z_1, blueshift z_2, and the radius of the emitter r_e. These results could help in testing conformal gravity by employing real astrophysical systems.

Furthermore, it would be interesting to estimate (or constraint) the free parameters N and l with the help of real astrophysical data of supermassive black holes hosted at the core of AGNs by making use of Bayesian fitting methods and comparing results to the previous estimations based on X-ray data [34, 35]. In addition, with the aim of constructing a more general astrophysical model, further extensions of this general relativistic approach would be of great interest, such as considering more general orbits (*i.e.* non-circular orbits and/or non-equatorial orbits) and incorporating the recessional motion of the host galaxy.

Within this general relativistic formalism, the detector recieves the information of spacetime background encoded in the frequency shift of photons emitted by the light source. Therefore, generalizing this formalism to general spherically symmetric spacetimes is a crucial extension of this approach and could be useful to extract information on black hole parameters and test extended theories of gravity.

Appendix A

Curvature invariants in conformal gravity

In Chapter 1, it has been stated that the black hole spacetime in conformal gravity is nonsingular. This statement is partially supported by the regularity of the Riemann tensor and curvature invariants, namely, the Kretschmann scalar and the Ricci scalar. In this appendix, we study this topic in more detail by computing these curvature scalars. We start by introducing the Riemann curvature tensor since the Ricci scalar and the Kretschmann scalar are constructed from contractions of the Riemann tensor, defined as follows

$$R_{\alpha\beta\gamma\delta} = \partial_\gamma \Gamma_{\alpha\delta\beta} - \partial_\delta \Gamma_{\alpha\gamma\beta} - \Gamma_{\alpha\gamma\nu}\Gamma^{\nu}{}_{\delta\beta} + \Gamma_{\alpha\delta\nu}\Gamma^{\nu}{}_{\gamma\beta}, \tag{A.1}$$

where we used the Christoffel symbol of the first kind

$$\Gamma_{\alpha\beta\gamma} = \frac{1}{2}(\partial_\beta \hat{g}_{\alpha\gamma} + \partial_\gamma \hat{g}_{\alpha\beta} - \partial_\alpha \hat{g}_{\beta\gamma}), \tag{A.2}$$

and the Christoffel symbol of the second kind

$$\Gamma^{\alpha}{}_{\beta\gamma} = \frac{\hat{g}^{\alpha\rho}}{2}(\partial_\beta \hat{g}_{\rho\gamma} + \partial_\gamma \hat{g}_{\rho\beta} - \partial_\rho \hat{g}_{\beta\gamma}), \tag{A.3}$$

related to the Christoffel symbol of the first kind via $\Gamma^{\alpha}_{\beta\gamma} = \hat{g}^{\alpha\sigma}\Gamma_{\sigma\beta\gamma}$. For the case of conformal gravity, the metric components (1.14)-(1.17) yield the following expressions for the nonvanishing components of Christoffel symbol

$$\begin{aligned}
&\Gamma^t_{tr} = \left(\tfrac{4Nl^2}{r^2-l^2} + \tfrac{r_s}{r-r_s}\right)\tfrac{1}{2r}, \quad && \Gamma^r_{tt} = \tfrac{r-r_s}{2r^3}\left(4Nl^2\tfrac{r-r_s}{r^2-l^2} + r_s\right), \quad && \Gamma^r_{rr} = \tfrac{1}{2r}\left(\tfrac{4Nl^2}{r^2-l^2} - \tfrac{r_s}{r-r_s}\right), \\
&\Gamma^r_{\theta\theta} = -\tfrac{r-r_s}{2}\left(\tfrac{4Nl^2}{r^2-l^2} + 2\right), && \Gamma^r_{\varphi\varphi} = -\tfrac{r-r_s}{2}\left(\tfrac{4Nl^2}{r^2-l^2} + 2\right)\sin^2\theta, && \Gamma^\theta_{r\theta} = \tfrac{1}{2r}\left(\tfrac{4Nl^2}{r^2-l^2} + 2\right), \\
&\Gamma^\theta_{\varphi\varphi} = -\sin\theta\cos\theta, && \Gamma^\varphi_{r\varphi} = \tfrac{1}{2r}\left(\tfrac{4Nl^2}{r^2-l^2} + 2\right), && \Gamma^\varphi_{\theta\varphi} = \cot\theta,
\end{aligned} \tag{A.4}$$

where $r_s = 2M$. Hence, their partial derivatives read

$$\begin{aligned}
&\partial_r \Gamma^t_{tr} = -\left[\tfrac{4Nl^2(r^2-l^2)+8Nl^2r^2}{(r^2-l^2)^2} + \tfrac{r_s(2r-r_s)}{(r-r_s)^2}\right]\tfrac{1}{2r^2}, \quad && \partial_r \Gamma^r_{tt} = -\left(\tfrac{4Nl^2(r-r_s)}{r^2-l^2} + r_s\right)\left(\tfrac{2r-3r_s}{2r^4}\right) \\
& && \qquad + \tfrac{r-r_s}{2r^3}\left[\tfrac{4Nl^2(2rr_s-r^2-l^2)}{(r^2-l^2)^2}\right], \\
&\partial_r \Gamma^r_{rr} = \tfrac{1}{2r}\left[\tfrac{r_s(2r-r_s)}{(r-r_s)^2} - \tfrac{4Nl^2(r^2-l^2)+8Nl^2r^2}{(r^2-l^2)^2}\right], && \partial_r \Gamma^r_{\theta\theta} = \tfrac{4Nl^2r^2+4Nl^4-8Nl^2rr_s-2(r^2-l^2)^2}{2(r^2-l^2)^2}, \\
&\partial_r \Gamma^r_{\varphi\varphi} = \partial_r \Gamma^r_{\theta\theta}\sin^2\theta, && \partial_r \Gamma^\theta_{r\theta} = \partial_r \Gamma^\varphi_{r\varphi} = -\tfrac{1}{r^2}\left[\tfrac{2Nl^2(3r^2-l^2)}{(r^2-l^2)^2} + 1\right], \\
&\partial_\theta \Gamma^r_{\varphi\varphi} = -(r-r_s)\left(\tfrac{2Nl^2}{r^2-l^2} + 1\right)2\sin\theta\cos\theta, && \partial_\theta \Gamma^\theta_{\varphi\varphi} = \sin^2\theta - \cos^2\theta, \\
&\partial_\theta \Gamma^\varphi_{\theta\varphi} = -\csc^2\theta.
\end{aligned} \tag{A.5}$$

With the help of the relations (A.4) and (A.5), it is possible to compute the Riemann tensor (A.1) as follows

$$
\begin{aligned}
R_{trtr} &= -\left(1-\frac{l^2}{r^2}\right)^{2N} \frac{2[Nl^2(r^2-l^2)+2Nl^2r^2](r-r_s)+r_s(r^2-l^2)^2-2Nl^2r_s(r^2-l^2)}{r^3(r^2-l^2)^2},\\
R_{t\theta t\theta} &= \left(1-\frac{l^2}{r^2}\right)^{2N} \frac{(r-r_s)}{2r^2}\left[\frac{8Nl^2l^4(r-r_s)+2Nl^2r_s(r^2-l^2)+r_s(r^2-l^2)^2}{(r^2-l^2)^2}\right.\\
&\quad\left.+\frac{4Nl^2(r-r_s)(r^2-l^2)}{(r^2-l^2)^2}\right],\\
R_{t\varphi t\varphi} &= R_{t\theta t\theta}\sin^2\theta,\\
R_{r\theta r\theta} &= \left(1-\frac{l^2}{r^2}\right)^{2N}\left[\frac{8Nl^2r^3-10Nl^2r^2r_s-r_s(r^2-l^2)^2+2Nl^4r_s}{2(r^2-l^2)^2(r-r_s)}\right],\\
R_{r\varphi r\varphi} &= R_{r\theta r\theta}\sin^2\theta,\\
R_{\theta\varphi\theta\varphi} &= -\left(1-\frac{l^2}{r^2}\right)^{2N} r^2\left[\frac{[4N^2l^4+4Nl^2(r^2-l^2)](r-r_s)-r_s(r^2-l^2)^2}{r(r^2-l^2)^2}\right]\sin^2\theta.
\end{aligned} \tag{A.6}
$$

Then, in order to obtain the Ricci scalar, it is necessary to define the Ricci tensor

$$
R_{\alpha\beta} = \hat{g}^{\mu\nu}R_{\mu\alpha\nu\beta} = \hat{g}^{tt}R_{trtr}+\hat{g}^{tt}R_{t\theta t\theta}+\hat{g}^{rr}R_{r\theta r\theta}+\hat{g}^{tt}R_{t\varphi t\varphi}+\hat{g}^{rr}R_{r\varphi r\varphi}+\hat{g}^{\theta\theta}R_{\theta\varphi\theta\varphi}, \tag{A.7}
$$

whose components for conformal gravity are expressed as follows

$$
\begin{aligned}
R_{tt} &= \frac{2Nl^2(r-r_s)(4Nl^2(r-r_s)+r_s(3r^2-l^2)-r(r^2-l^2))}{r^4(r^2-l^2)^2},\\
R_{rr} &= \frac{2Nl^2(7r^3-l^2r+3l^2r_s-9r^2r_s)}{r^2(r^2-l^2)^2(r-r_s)},\\
R_{\theta\theta} &= -\frac{2Nl^2(4Nl^2r+2l^2r_s+r^3-3l^2r-4Nl^2r_s)}{r(r^2-l^2)^2},\\
R_{\varphi\varphi} &= R_{\theta\theta}\sin^2\theta.
\end{aligned} \tag{A.8}
$$

Therefore, the Ricci scalar reads

$$
R = \hat{g}^{\mu\nu}R_{\mu\nu} = \hat{g}^{tt}R_{tt}+\hat{g}^{rr}R_{rr}+\hat{g}^{\theta\theta}R_{\theta\theta}+\hat{g}^{\varphi\varphi}R_{\varphi\varphi}, \tag{A.9}
$$

hence, we obtain the following expression for the Ricci scalar

$$
R = \left(1-\frac{l^2}{r^2}\right)^{-2N}\frac{12Nl^2(r^3-2r^2r_s+l^2r-2Nl^2r+2Nl^2r_s)}{r^3(r^2-l^2)^2}, \tag{A.10}
$$

which reduces to

$$
R \approx \frac{24N^2}{l^{4N}}r^{4N-3} \tag{A.11}
$$

near the origin in the limit $r \to 0$. On the other hand, the Kretschmann scalar is defined in the following way

$$
\begin{aligned}
\mathcal{K} &= R^{\alpha\beta\gamma\delta}R_{\alpha\beta\gamma\delta} = \hat{g}^{\alpha\mu}\hat{g}^{\beta\nu}\hat{g}^{\gamma\rho}\hat{g}^{\delta\sigma}R_{\mu\nu\rho\sigma}R_{\alpha\beta\gamma\delta} = (\hat{g}^{tt}\hat{g}^{rr})^2R_{trtr}+(\hat{g}^{tt}\hat{g}^{\theta\theta})^2R_{t\theta t\theta}\\
&\quad+(\hat{g}^{rr}\hat{g}^{\theta\theta})^2R_{r\theta r\theta}+(\hat{g}^{tt}\hat{g}^{\varphi\varphi})^2R_{t\varphi t\varphi}+(\hat{g}^{rr}\hat{g}^{\varphi\varphi})^2R_{r\varphi r\varphi}+(\hat{g}^{\theta\theta}\hat{g}^{\varphi\varphi})^2R_{\theta\theta\varphi\varphi},
\end{aligned} \tag{A.12}
$$

which has the following explicit form

$$\mathcal{K} = \left(1 - \frac{l^2}{r^2}\right)^{-4N} \frac{4}{r^6(r^2-l^2)^4} \left(3r^8 r_s^2 - 12l^2 r^6 r_s^2 + 48N^4 l^8 (r-r_s)^2 + 3l^8 r_s^2 - 64N^3 l^8 r^2\right.$$
$$+112N^3 l^8 r r_s - 48N^3 l^8 r_s^2 + 28N^2 l^8 r^2 - 56N^2 l^8 r r_s + 36N^2 l^8 r_s^2 - 12l^6 r^2 r_s^2 + 64N^3 l^6 r^4$$
$$-112N^3 l^6 r^3 r_s + 48N^3 l^6 r^2 r_s^2 - 72N^2 l^6 r^4 + 176N^2 l^6 r^3 r_s - 120N^2 l^6 r^2 r_s^2 + 18l^4 r^4 r_s^2$$
$$\left. + 92N^2 l^4 r^6 - 216N^2 l^4 r^5 r_s + 132N^2 l^4 r^4 r_s^2\right), \tag{A.13}$$

and can be approximated as follows

$$\mathcal{K} \approx \frac{12}{l^{8N}}(1 + 12N^2 - 16N^3 + 16N^4) r^{8N-6}, \tag{A.14}$$

for $r \to 0$. Now, from Eqs. (A.11) and (A.14), we see that the Ricci scalar and the Kretschmann scalar are regular at the center of the conformal gravity black holes for $N \geq 1$ and $l \neq 0$, unlike the Schwarzschild solution.

Bibliography

1. Hobson, M., Efstathiou, G. & Lasenby, A. *General Relativity: An Introduction for Physicists* ISBN: 9780521829519. https://books.google.com.mx/books?id=5dryXCWR7EIC (Cambridge University Press, 2006).
2. Rindler, W. *Relativity: Special, General, and Cosmological* ISBN: 9780198508359. https://books.google.com.mx/books?id=fUj%5C_LW51GfQC (Oxford University Press, 2001).
3. Penrose, R. Gravitational Collapse and Space-Time Singularities. *Phys. Rev. Lett.* **14,** 57–59. https://link.aps.org/doi/10.1103/PhysRevLett.14.57 (1965).
4. Schmidt, M. 3C 273 : A Star-Like Object with Large Red-Shift. *Nature* **197,** 1040–1040. ISSN: 1476-4687. https://doi.org/10.1038/1971040a0 (1963).
5. Oppenheimer, J. R. & Snyder, H. On Continued Gravitational Contraction. *Phys. Rev.* **56,** 455–459. https://link.aps.org/doi/10.1103/PhysRev.56.455 (1939).
6. Eckart, A. & Genzel, R. Observations of stellar proper motions near the Galactic Centre. *Nature* **383,** 415–417. ISSN: 1476-4687. https://doi.org/10.1038/383415a0 (1996).
7. Ghez, A. M. *et al.* Measuring Distance and Properties of the Milky Way's Central Supermassive Black Hole with Stellar Orbits. *Astrophys. J.* **689,** 1044. https://dx.doi.org/10.1086/592738 (2008).
8. Gillessen, S. *et al.* Monitoring stellar orbits around the massive black gole in the galactic center. *Astrophys. J.* **692,** 1075. https://dx.doi.org/10.1088/0004-637X/692/2/1075 (2009).
9. Collaboration, E. H. T. *et al.* First Sagittarius A* Event Horizon Telescope Results. VI. Testing the Black Hole Metric. *Astrophys. J. Lett.* **930,** L17. https://dx.doi.org/10.3847/2041-8213/ac6756 (2022).
10. Collaboration, T. E. H. T. *et al.* First M87 Event Horizon Telescope Results. IV. Imaging the Central Supermassive Black Hole. *Astrophys. J. Lett.* **875,** L4. https://dx.doi.org/10.3847/2041-8213/ab0e85 (2019).
11. Abbott, B. P. *et al.* GW151226: Observation of Gravitational Waves from a 22-Solar-Mass Binary Black Hole Coalescence. *Phys. Rev. Lett.* **116,** 241103. https://link.aps.org/doi/10.1103/PhysRevLett.116.241103 (2016).
12. Abbott, B. P. *et al.* Observation of Gravitational Waves from a Binary Black Hole Merger. *Phys. Rev. Lett.* **116,** 061102. https://link.aps.org/doi/10.1103/PhysRevLett.116.061102 (2016).
13. Herrera-Aguilar, A. & Nucamendi, U. Kerr black hole parameters in terms of the redshift/blueshift of photons emitted by geodesic particles. *Phys. Rev. D* **92,** 045024. https://link.aps.org/doi/10.1103/PhysRevD.92.045024 (2015).
14. Banerjee, P., Herrera-Aguilar, A., Momennia, M. & Nucamendi, U. Mass and spin of Kerr black holes in terms of observational quantities: The dragging effect on the redshift. *Phys. Rev. D* **105,** 124037. https://link.aps.org/doi/10.1103/PhysRevD.105.124037 (2022).

15. Momennia, M., Herrera-Aguilar, A. & Nucamendi, U. Kerr black hole in de Sitter spacetime and observational redshift: Toward a new method to measure the Hubble constant. *Phys. Rev. D* **107,** 104041. https://link.aps.org/doi/10.1103/PhysRevD.107.104041 (2023).

16. Martínez-Valera, D. A., Momennia, M. & Herrera-Aguilar, A. Observational redshift from general spherically symmetric black holes. arXiv: 2311.17993 [gr-qc] (2023).

17. Momennia, M., Banerjee, P., Herrera-Aguilar, A. & Nucamendi, U. Schwarzschild black hole and redshift rapidity: A new approach towards measuring cosmic distances. arXiv: 2312.07426 [gr-qc] (2023).

18. Fu, Q.-M. & Zhang, X. Probing a polymerized black hole with the frequency shifts of photons. *Phys. Rev. D* **107,** 064019. https://link.aps.org/doi/10.1103/PhysRevD.107.064019 (2023).

19. Nucamendi, U., Herrera-Aguilar, A., Lizardo-Castro, R. & López-Cruz, O. Toward the Gravitational Redshift Detection in NGC 4258 and the Estimation of Its Black Hole Mass-to-distance Ratio. *Astrophys. J. Lett.* **917,** L14. ISSN: 2041-8213. http://dx.doi.org/10.3847/2041-8213/ac151b (2021).

20. Villalobos-Ramírez, A., Gallardo-Rivera, O., Herrera-Aguilar, A. & Nucamendi, U. A general relativistic estimation of the black hole mass-to-distance ratio at the core of TXS 2226–184. *Astron. Astrophys.* **662,** L9. ISSN: 1432-0746. http://dx.doi.org/10.1051/0004-6361/202243653 (2022).

21. Villaraos, D., Herrera-Aguilar, A., Nucamendi, U., González-Juárez, G. & Lizardo-Castro, R. A general relativistic mass-to-distance ratio for a set of megamaser AGN black holes. *MNRAS* **517,** 4213–4219. ISSN: 1365-2966. http://dx.doi.org/10.1093/mnras/stac2973 (2022).

22. Villalobos-Ramírez, A., González-Juárez, A., Momennia, M. & Herrera-Aguilar, A. A general relativistic mass-to-distance ratio for a set of megamaser AGN black holes II. arXiv: 2211.06486 [astro-ph.GA] (2022).

23. Kroon, J. A. V. *Conformal Methods in General Relativity* (Cambridge University Press, 2023).

24. Hölscher, P. *Conformal Gravity* MA thesis (Bielefeld University, 2015). https://www2.physik.uni-bielefeld.de/fileadmin/user_upload/theory_e6/Master_Theses/Masterarbeit_PatricHoelscher.pdf.

25. Narlikar, J. V. & Kembhavi, A. K. Space-time singularities and conformal gravity. *Lett. Nuovo Cim.* **19,** 517–520. ISSN: 1827-613X. https://doi.org/10.1007/BF02748215 (1977).

26. Bambi, C., Modesto, L. & Rachwał, L. Spacetime completeness of non-singular black holes in conformal gravity. *JCAP* **2017,** 003. https://dx.doi.org/10.1088/1475-7516/2017/05/003 (2017).

27. Toshmatov, B., Bambi, C., Ahmedov, B., Abdujabbarov, A. & Stuchlık, Z. Energy conditions of nonsingular black hole spacetimes in conformal gravity. *Eur Phys. J. C* **77,** 1–10 (2017).

28. Papoyan, V., Pervushin, V. & Smirichinskii, V. Conformally invariant model of the early universe. *Astrophys.* **41,** 299–307 (1998).

29. Hinterbichler, K. & Khoury, J. The pseudo-conformal universe: scale invariance from spontaneous breaking of conformal symmetry. *JCAP* **2012,** 023–023. ISSN: 1475-7516. http://dx.doi.org/10.1088/1475-7516/2012/04/023 (2012).

30. Modesto, L. & Rachwal, L. Finite Conformal Quantum Gravity and Nonsingular Spacetimes. arXiv: 1605.04173 [hep-th] (2016).

31. Chen, C.-Y. & Chen, P. Gravitational perturbations of nonsingular black holes in conformal gravity. *Phys. Rev. D* **99,** 104003. https://link.aps.org/doi/10.1103/PhysRevD.99.104003 (2019).

32. Grøn, Ø. & Hervik, S. *Einstein's General Theory of Relativity: With Modern Applications in Cosmology* ISBN: 9780387691992. https://books.google.com.mx/books?id=COqUEa5M6O0C (Springer New York, 2007).
33. Carroll, S. M. *Spacetime and geometry* (Cambridge University Press, 2019).
34. Bambi, C., Cao, Z. & Modesto, L. Testing conformal gravity with astrophysical black holes. *Phys. Rev. D* **95,** 064006. https://link.aps.org/doi/10.1103/PhysRevD.95.064006 (2017).
35. Zhou, M. *et al.* Testing conformal gravity with the supermassive black hole in 1H0707-495. *Phys. Rev. D* **98,** 024007. https://link.aps.org/doi/10.1103/PhysRevD.98.024007 (2018).
36. Uspensky, J. *Theory of Equations* (McGraw-Hill, 1948).